17th World Conference on Earthquake Engineering, 17WCEE
Sendai, Japan – September 13th to 18th 2020

Multi-layer Seismic Isolation Building with Base-isolated Core

K. Sugimoto[(1)], S. Ushizaka[(2)], S. Kotsuki[(3)] and K. Isoda[(4)]

[(1)] *Research Engineer, Institute of Technology, Shimizu Corporation, M.Eng. k_sugimoto@shimz.co.jp*
[(2)] *Structural Engineer, Design Division, Shimizu Corporation, M.Eng. ushizaka_s@shimz.co.jp*
[(3)] *Senior Research Engineer, Institute of Technology, Shimizu Corporation, Dr.Eng. sachie.yamamoto@shimz.co.jp*
[(4)] *Chief Research Engineer, Institute of Technology, Shimizu Corporation, M.Eng. isoda@shimz.co.jp*

Abstract

We propose a new seismic isolation system that realizes better building performance against earthquakes than the conventional base-isolated structure. The target performance is that the response acceleration of all layers should be 100 cm/s^2 or less and the interlayer deformation angle of all layers should be 1/400 or less for Level 2 ground motion. This proposed seismic isolation system has multiple seismic isolation layers and a base-isolated core wall.

We first construct a two-degree-of-freedom model of this system in order to study the isolation specifications that can be expected to achieve effective reduction of earthquake response. The findings of this study using complex eigenvalue analysis and frequency transfer functions are the following.

1) By increasing the damping of the core base-isolation layer, it is possible to increase only the first-order damping factor without causing second-order overdamping. This means that a significant response reduction effect can be expected in the resonance region as compared with a multi-layer seismic isolation frame without a base-isolated core.

2) It is possible to reduce the response on the short period side by adjusting the stiffness ratio of each seismic isolation layer.

Next, we construct a multi-degree-of-freedom model based on the above results and carry out earthquake response analysis. For input motion, we design ground motions according to the notifications of the Japanese building codes equivalent to Level 2 motion as well as a motion based on the anticipated Nankai-Trough earthquake that exceeds Level 2. The analysis shows the target performance is achieved for Level 2 seismic motion. Moreover, the superiority of this system is confirmed even for seismic waves exceeding Level 2.

Keywords: base-isolated structure; mult-layer seismic isolation; super high-rise building; earthquake response analysis; complex eigenvalue analysis

1. Introduction

In recent years, it has become clear that higher levels of ground motion need to be considered in building design, as demonstrated by the Pacific Coast of Tohoku Earthquake [1],[2]. In addition, from the perspective of Business Continuity Planning, society is demanding high value-added buildings with seismic isolation and improved safety and seismic margins. The authors have proposed a frame design based on the new concept of seismic isolation layers and with an additional seismic isolation layer under a core structure that penetrates the whole building. It has already been shown that this proposed frame reduces earthquake response more effectively than the conventional seismic isolation frame and a seismic isolation structure with multiple seismic isolation layers [3],[4],[5]. In this paper, we examine the feasibility of setting certain performance targets for this structure – acceleration less than 100 cm/s^2 for all stories of a building and seismic isolation layer deformations less than the guaranteed performance of the isolation material – under Level 2 earthquake ground motion. First, we prepare a two-degree-of-freedom model of the proposed frame and, using complex eigenvalue analysis and frequency transfer functions, determine seismic isolation parameters that reduce the response to a lower level than conventional seismic isolation structures. Next, using the seismic isolation parameters obtained, we create a multi-degree-of-freedom model and conduct seismic response analysis to investigate the feasibility of the performance targets.

2. Target building model

Figure 1 shows a conceptual diagram of the proposed frame. This is essentially a malti-layer seismic isolation system with seismic isolation layers at the base and part way up the structure. In addition, a core wall integrated with the upper section of the structure penetrates the entire building and has an additional seismic isolation layer at its foundation. This core wall secures a vertical traffic line for building users and seismic force can be transmitted as if a through a mandrel. In order to examine the response reduction effect of this proposed frame, we also examine a simple two-layer seismic isolation frame (multi-layer frame) for comparison. Figure 2 shows a conceptual diagram of this multi-layer frame. In both frames, the section above the middle seismic isolation layer is defined as mass point A (upper floors) and the section below is defined as mass point B (lower floors). We represent these frames using two-degree-of-freedom shear models. In the model of Figure 2, the parameters k_3 and c_3 are set to 0 for a multi-layer frame. Figure 3 shows the two-degree-of-freedom shear model and the first order vibration mode of both analysis models. Here, assuming that the eigenvectors of the mass points A and B are r_1 and r_2, respectively, the eigenvector ratio based on r_1 is defined as $\gamma(r_2/r_1)$. The masses of mass points A and B are defined as M_A and M_B, and the mass ratio (M_B/M_A) is defined as μ. The stiffness of the base seismic isolation layer, the middle seismic isolation layer, and the seismic isolation layer below the core are defined as k_1, k_2, and k_3, and the rigidity ratios of k_2 and k_3 to k_1 are defined as α and β. In this work, the core wall is assumed rigid.

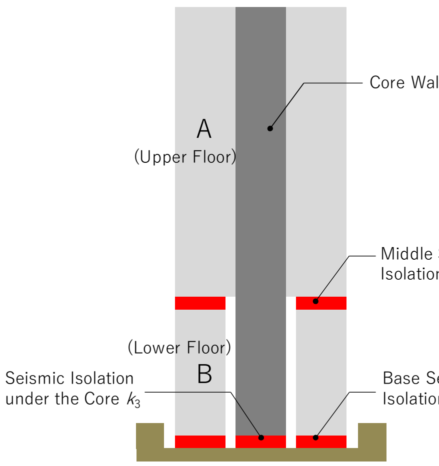

Fig. 1 Conceptual diagram of the proposed frame

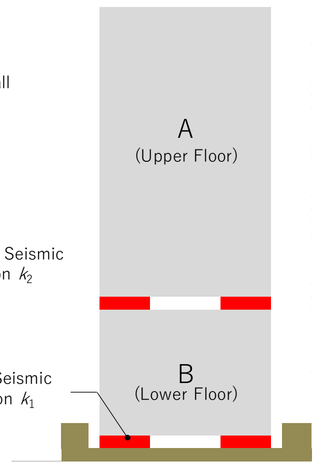

Fig. 2 Conceptual diagram of the multi-layer frame

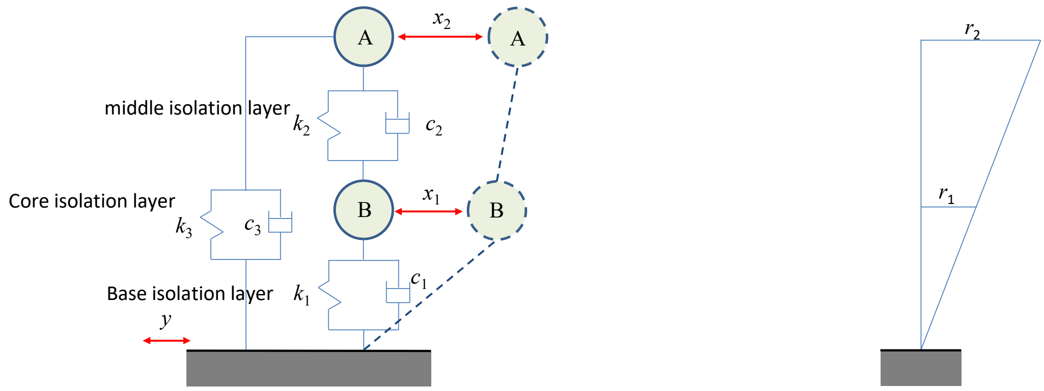

Fig. 3 Two-degree-of-freedom analysis model and primary vibration mode

3. Seismic isolation specifications and response reduction effect of the proposed frame

The features of the proposed frame are that the core wall, which is integrated with mass point A, penetrates all layers and that the core has a base seismic isolation layer. The deformation of the base-isolation layer under the core wall (k_3) is the summed deformation of the two seismic isolation layers (the base isolation layer and the middle seismic isolation layer). The damping device (c_3) installed in that layer can absorb a large amount of energy. In this chapter, we consider the response reduction effect of damping device (c_3) and the effective rigidity ratio of each seismic isolation layer of the proposed frame.

3.1 Damping under the core wall

We perform complex eigenvalue analysis with damping coefficients c_1, c_2, and c_3 of the three seismic isolation layers as parameters using the two-degree-of-freedom model in Figure 3. Then we examine the effect of changing each damping coefficient on the change of the first order and second order damping factors.

In the analysis model, the mass ratio is set to 1.0, and the first order natural period is set to 7.0 seconds. Furthermore, the stiffness of the base seismic isolation layer (k_1) and that of the middle seismic isolation layer (k_2) are set such that the deformation of the base seismic isolation layer and the middle seismic isolation layer in the first order vibration mode is the same (γ= 2). As initial states for c_1 and c_2, the damping factor is set to 20% for the first order natural period. Then c_1, c_2, and c_3 are changed from the initial state by 0 to 1.0 times the initial value of c_1. Figures 4 (a)-(c) show the results of this analysis. It can be seen that when c_3 is increased, the first order damping factor (h_1) rises significantly as compared with the case when c_1 and c_2 increased. On the other hand, the second order damping factor (h_2) does not change significantly even when c_3 is increased. This result indicates that, by increasing c_3, the first order damping factor only can be greatly increased without second-order overdamping. In other words, first order vibration can be significantly reduced by installing more damping in the seismic isolation layer under the core wall as in the proposed frame.

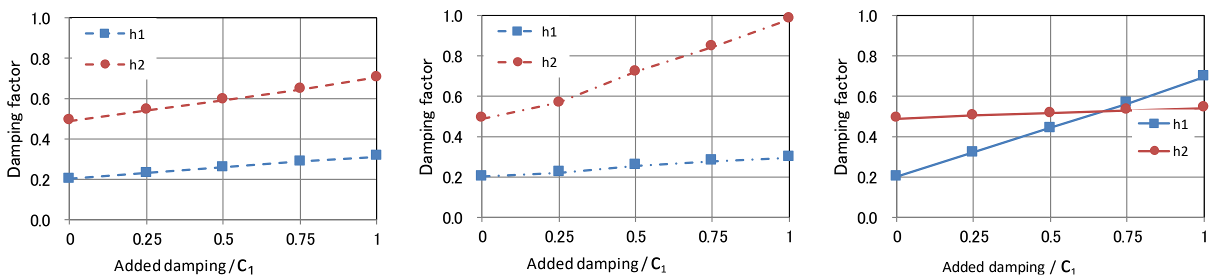

(a) c_1 is changed (b) c_2 is changed (c) c_3 is changed

Fig. 4 Variation in damping constant when each damping coefficient is changed

3.2 Stiffness ratio of seismic isolation layer

We study the effect of varying the stiffness ratio of each seismic isolation layer using the two-degree-of-freedom model. By changing the stiffness of each seismic isolation layer and comparing the frequency transfer functions of displacement and acceleration, we obtain stiffness ratios result in effective response reduction.

Table 1 shows the specifications of the four analysis models that are compared. The first order natural period of each model is set at 7.0 seconds, and the four cases are implemented using eigenvector ratios. The models in which deformation of the base seismic isolation layer and the middle seismic isolation layer is the same (Case1, Case2; γ = 2) are taken to be the standard. Case1 is the multi-layer frame and Case2 is the proposed frame. The model in which mass A is displaced more than mass B is named Case3 (γ = 3), while the model in which mass A is displaced less than mass B is Case4 (γ = 1.4). All stiffness ratios given in the table are relative to k_1 in Case1.

Here, defining the displacement of mass point A as x_2, the displacement of mass point B as x_1, and the ground motion input acceleration as y in the analysis model shown in Fig. 3, the vibration equation given by formula (1) can be constructed. Then, by solving the eigenvalue problem represented by formula (2), formulas (3) and (4) arranged in terms of eigenvector ratio γ are obtained. Formula (5) expresses γ using formulas (3) and (4). The definitions of α, β, μ, and γ are as given in section 2 above. Furthermore, the first natural period T of the proposed frame can be expressed using formula (7) in terms of period T_A of the system consisting of mass point A and stiffness k_2 of the middle seismic isolation layer, and κ consisting of α, β and γ. κ represents the increment in natural period brought about only by the seismic isolation system in the middle layer of the proposed frame. The seismic isolation data given in Table 1 is calculated using formula (5). The damping in Case1 is set such that c_1 and c_2 provide 20% proportional damping with respect to the first order natural period. As for damping in Case2 to Case4, c_3 is set to 80% of the value of c_2 in Case1. This is because the results in section 3.1 showed that the response reducing effect of c_3 was large. The value of c_1 in Case1 to Case4 is not changed.

Table 1 Specifications of model for analysis

μ = 1.0 (μ : mass ratio)		Multi-layer	Proposed frame		
		Case1	Case2	Case3	Case4
Eigenvector ratios	γ	2	2	3	1.4
Increment in natural period	κ	1.41	1.09	0.9	1.31
Natural period [s]	T	7.00	7.00	7.00	7.00
Stiffness Ratio (Based on k_1)	k_1	1.00	1.10	1.20	0.83
	k_2	0.66	0.65	0.42	0.83
	k_3	0.00	0.22	0.24	0.25
	α	0.67	0.59	0.35	1.00
	β	0.00	0.20	0.20	0.30
Damping Factor (Based on c_1)	c_1	1.00	1.00	1.00	1.00
	c_2	0.67	0.13	0.13	0.13
	c_3	0.00	0.54	0.54	0.54

$$\begin{bmatrix} M_A & 0 \\ 0 & M_B \end{bmatrix} \begin{Bmatrix} \ddot{x}_2 \\ \ddot{x}_1 \end{Bmatrix} + \begin{bmatrix} k_3 + k_2 & -k_2 \\ -k_2 & k_2 + k_1 \end{bmatrix} \begin{Bmatrix} x_2 \\ x_1 \end{Bmatrix} = - \begin{bmatrix} M_A & 0 \\ 0 & M_B \end{bmatrix} \begin{Bmatrix} 1 \\ 1 \end{Bmatrix} \ddot{y} \quad \text{... (1)}$$

$$\begin{bmatrix} k_3 + k_2 - \omega^2 M_A & -k_2 \\ -k_2 & k_2 + k_1 - \omega^2 M_B \end{bmatrix} \begin{Bmatrix} \gamma_2 \\ \gamma_1 \end{Bmatrix} = \begin{Bmatrix} 0 \\ 0 \end{Bmatrix} \quad \text{... (2)}$$

$$\frac{r_2}{r_1} = \frac{k_2}{k_3+k_2-\omega^2 M_A} \quad \text{... (3)} \qquad \frac{r_2}{r_1} = \frac{k_2+k_1-\omega^2 M_B}{k_2} \quad \text{... (4)}$$

$$\gamma = \frac{-\{-\alpha-1+(\alpha+\beta)\mu\}\pm\sqrt{\{-\alpha-1+(\alpha+\beta)\mu\}^2+4\alpha^2\mu}}{2\alpha} \quad \text{... (5)}$$

$$\omega^2 = \frac{k_2}{m_A}\left(\frac{\beta}{\alpha}+1-\frac{1}{\gamma}\right) \quad \text{... (6)}$$

$$T = \kappa \cdot T_A \quad \text{... (7)}$$

Here, because $T_A = 2\pi\sqrt{\frac{M_A}{k_2}}$,

$$\kappa = \sqrt{\frac{\gamma}{(\beta/\alpha+1)\gamma-1}} \quad \text{... (8)}$$

We calculate the frequency transfer function for displacement and acceleration of each mass point for Case1 to Case4, and the results are shown in Figures 5 (a)-(d). From (a) and (c) it can be seen that, compared with the multi-layer frame of Case1, the displacement and acceleration of mass point A in the proposed frame are significantly reduced to about 50% in all cases. This is probably because the first-order damping factor is increased by the application of damping c_3 in the core isolation layer of the proposed frame. From (b) and (d), it can be seen that the larger the value of γ, the more the secondary displacement and acceleration responses of mass point B are excited. The target acceleration of the proposed frame is set at 100m/s^2 or less in all layers for Level 2 earthquake ground motion, so it is important to reduce the higher mode response as this greatly affects acceleration. Therefore, as in Case4 in Figure 5 (d), it is desirable to suppress secondary vibration of mass point B, so we set $1.0 < \gamma < 2.0$ as the effective range of γ in the proposed frame.

From the above results, the relationships between α and β for a mass ratio set to 0.5 and 1.0 are calculated using formulas (5) and (8). These are shown in Fig. 6 (a) and (b). The shaded areas in Fig. 6 indicate the stiffness ratios with which the response of the proposed frame is effectively reduced. Here, we set κ>1.0 in order to ensure that the period is longer than that of the normal seismic isolation frame. In addition, considering the surface pressure on the laminated rubber, we set $\alpha \leqq 1.0$. This is because the stiffness of the base seismic isolation layer, which supports a greater weight, is larger than that of the middle seismic isolation layer.

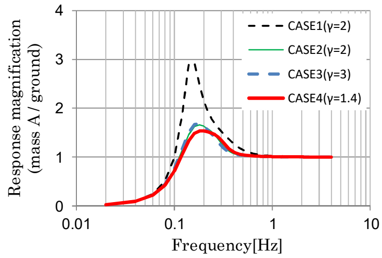

(a) Displacement of mass point A

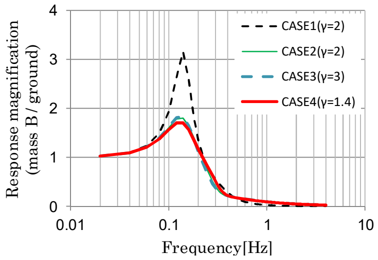

(b) Displacement of mass point B

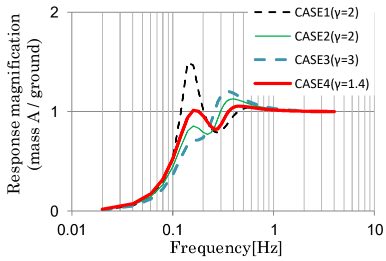

(c) Acceleration of mass point A

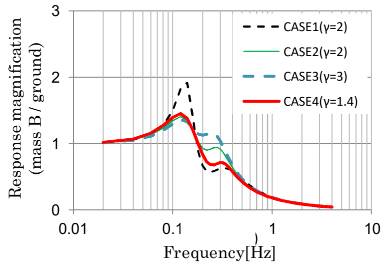

(d) Acceleration of mass point B

Fig. 5 Frequency transfer functions

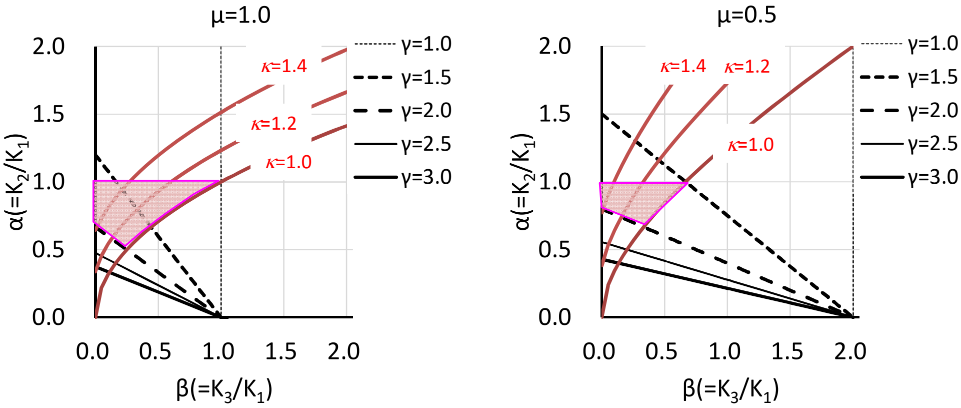

(a) Mass ratio $\mu = 1.0$ (b) Mass ratio $\mu = 0.5$

Fig. 6 Effective ranges of α and β

4. Earthquake response analysis using multi-degree-of-freedom model

We create a multi-degree-of-freedom model of a frame with the seismic isolation specification proposed in section 3 and use it to conduct seismic response analysis. The target building is a skyscraper with 31 above-ground floors. We assume a complex consisting of two large volumes, one (part B; the lower floors) comprising the 1st to 3rd floors and the other (part A; upper floors) consisting of the 4th to 31st floors. For comparison and to demonstrate the effectiveness of the proposed frame design, the equivalent multi-layer frame and normal seismic isolation are also modeled. In the multi-layer frame, the core part does not penetrate all layers but is separated by the middle seismic isolation layer. Normal seismic isolation means a structure in which the lower floors are an earthquake-resistant structure with an intermediate seismic isolation layer above them.

4.1 Analytical models

Equivalent shear multi-degree-of-freedom models are developed for analysis, as shown in Figures 7(a)-(c). The proposed frame, shown in Figure 7(a), includes one part (A) representing the core and upper floors; this is connected to the base seismic isolation at the bottom and to the upper floors. The lower floor part (B) includes the base seismic isolation connects to the middle layer seismic isolation. The multi-layer frame and the normal seismic isolation models are illustrated in Figures 7 (b) and (c), respectively.

Table 2 shows the seismic isolation layer specifications of each model. The seismic isolation layer stiffness of the proposed frame structure and the multi-layer frame structure is represented by eigenvector ratios γ obtained by replacing the two mass systems; the values are $\gamma = 1.77$ and $\gamma = 2.0$, respectively. Also, the primary natural period is set to about 7.5 seconds. On the other hand, the normal seismic isolation model has a bilinear restoring force characteristic that assumes the use of a steel damper and natural rubber. The first natural period is set to 5.0 seconds at 200% seismic isolation layer strain. In addition, the restoring force characteristics of the proposed frame and the multi-layer frame are linear with natural rubber and oil dampers.

For damping, we allow 2% damping in proportion to stiffness as structural damping. In the multi-layer frame, the first damping factor of the seismic isolation layers is viscous damping set at about 12%. In the proposed frame, the seismic isolation layer under the core has viscous damping of 50,000 [kNs/m], and the other seismic isolation layers are arranged so as to have the same amount of attenuation as in the multi-layer frame. On the other hand, the viscous damping of the normal seismic isolation model is set such that the first order damping coefficient as total of hysteretic damping, obtained by equivalent linearization, and viscous damping, is about 12%. In each model, oil dampers are assumed for viscous damping, with a relief speed of 0.32 m/s and a bilinear characteristic.

The seismic isolation parameters set for the proposed frame are μ = 0.41, α = 1.0, β = 0.12, and γ = 1.77. These were confirmed to be within the range of effective response reduction shown in section 3 (Figure 8). Figures 9 (a)-(c) show the natural period and stimulus function for each model. In the proposed frame and the multi-layer frame, the participation vectors of the middle seismic isolation layer and the base seismic isolation layer are almost the same as expected. Further, in the proposed frame, the second order participation vector is relatively smaller than in the other models and, as shown in Figure 5, vibrates mainly in the first mode in the range of 1.0 < γ < 2.0.

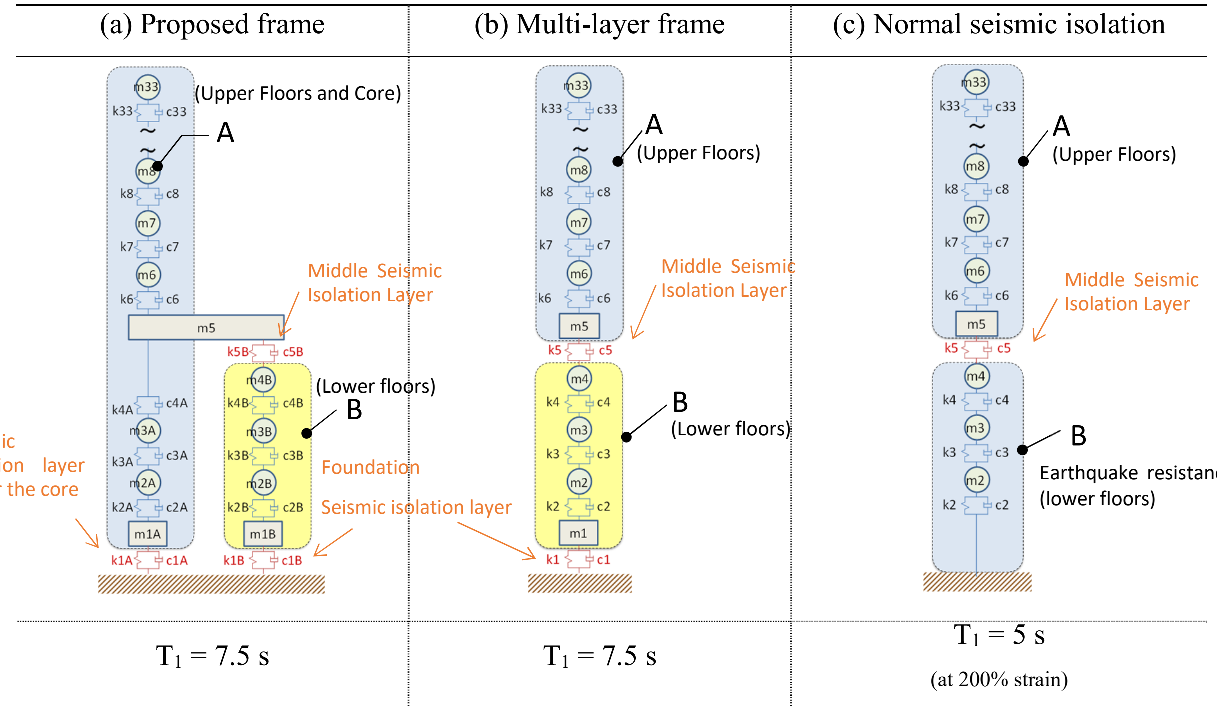

Fig. 7 Multi-degree-of-freedom models

Table 2 Seismic isolation layer specifications of each model

Model	Proposed frame		Multi-layer frame		Normal seismic isolation	
	Stiffness [kN/cm]	Viscous damping [kNs/m]	Stiffness [kN/cm]	Viscous damping [kNs/m]	Stiffness [kN/cm]	Viscous damping [kNs/m]
Intermediate seismic isolation	1600	30000	1756	57500	2275	25000
Base isolation	1600	50000	2200	72500	-	-
Lower-core Base isolation	189	50000	-	-	-	-

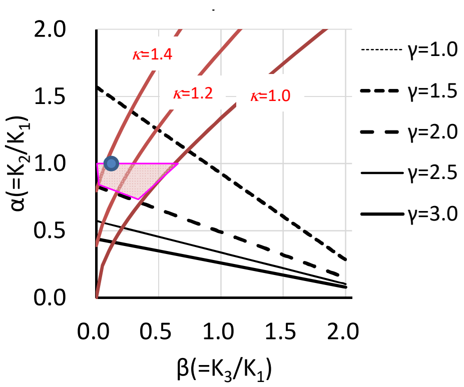

Fig. 8 Seismic isolation specifications of the proposed frame ($\mu = 0.41$)

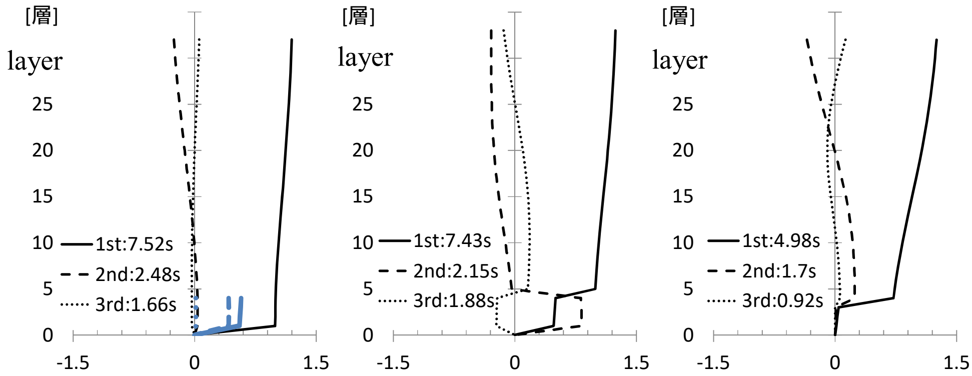

(a) Proposed frame (b) Multi-layer frame (c) Normal seismic isolation

Fig. 9 Stimulus function

4.2 Input ground motion

Five different input ground motions are used for time history response analysis. The first is a ground motion, using random phase, fitted to the Level 2 design response spectrum. The second is a ground motion, using the phase of the observed record at Kobe station during the 1995 Kobe earthquake, fitted to the Level 2 design response spectrum. The third and fourth motions, representing earthquakes exceeding Level 2, are the area OS1 and CH1 waveforms assuming the Nankai Trough Earthquake[6]. The fifth waveform is the EW motion observed at Mashiki-cho, Miyazono during the main shock of the 2016 Kumamoto earthquake[7]. Figure 10 shows the pseudo-velocity response spectra of these five seismic waveforms.

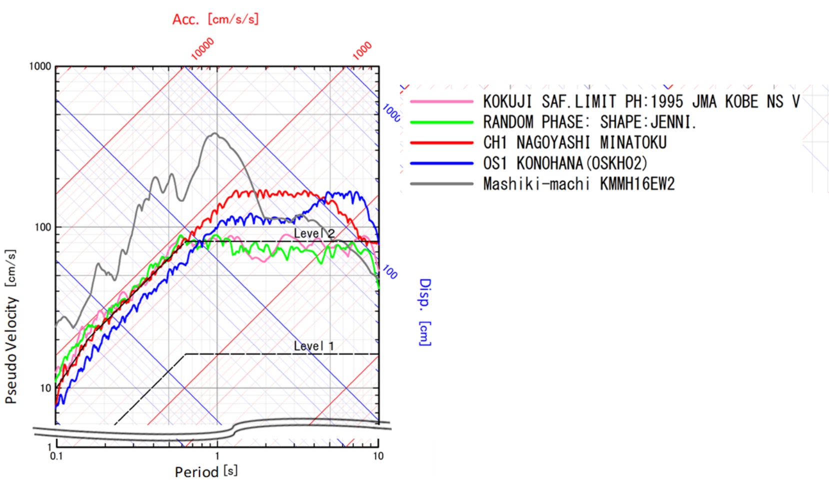

Fig. 10 Pseudo-velocity response spectrum of input ground motions

4.3 Analysis results

Figure 11 shows the maximum response accelerations and Fig. 12 shows the maximum interlayer deformation angle. Looking at the maximum response accelerations shown in Fig. 11, the proposed frame achieves a maximum of 100 cm/s^2 or less in all layers against OS1 and the two waveforms standardized to Level 2. This is because the first natural period is increased and the damping is concentrated in the seismic isolation layer under the core. On the other hand, the CH1 and Mashiki-cho ground motions, which contain many short-period components of less than 2 seconds, result in accelerations that slightly exceed 100cm/s^2 at the lower floors (part B) and at the top floor. Further, regarding the interlayer deformation angle shown in Figure 12, it was 1/400 or less for all layers of the proposed frame against the ground motion of all five waveforms. Figure 13 shows the maximum response deformation of each seismic isolation layer in each model for all input motions. In the proposed frame, seismic isolation layer deformation at the base and middle layers is less than 250 mm for the design ground motion. The Mashiki-cho, Miyazono EW motion results in the largest deformation, 398 mm. These results are less than the 500 mm guaranteed deformation performance obtained assuming a total laminated rubber thickness of 200 mm. The deformation of the base seismic isolation layer under the core is a maximum of 708 mm under OS1 ground motion. This is within the guaranteed deformation performance of 800 mm assuming a total rubber thickness of 320 mm.

Figure 14 shows the relative response deformation waveforms of the base seismic isolation layer under the core and the base seismic isolation layer when the JMA Kobe NS phase is applied to the proposed frame. The two seismic isolation layers always move with almost the same phase and, if appropriate clearance is secured around the core, the core does not collide with the lower floors.

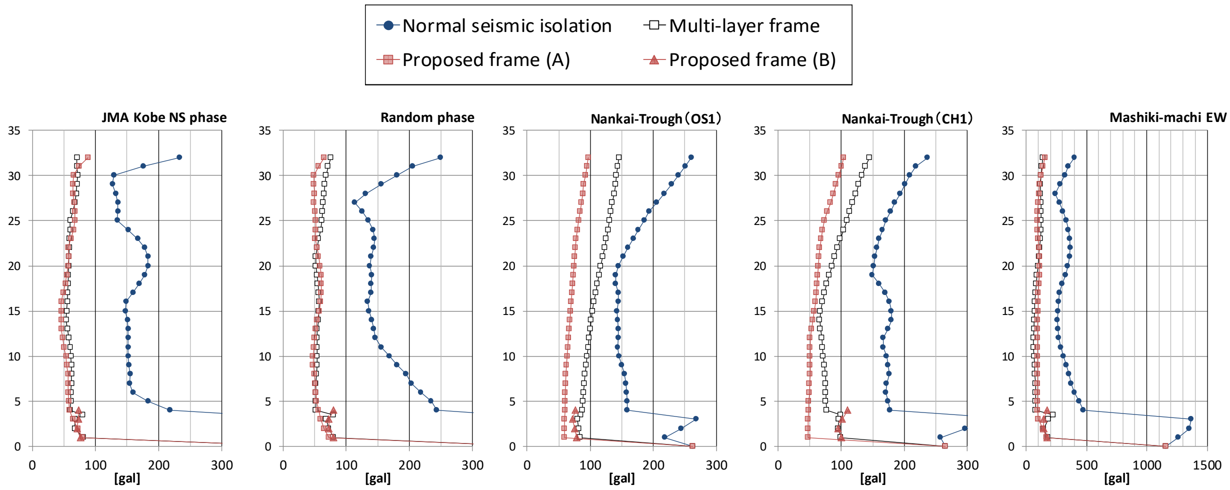

Fig. 11 Maximum response acceleration

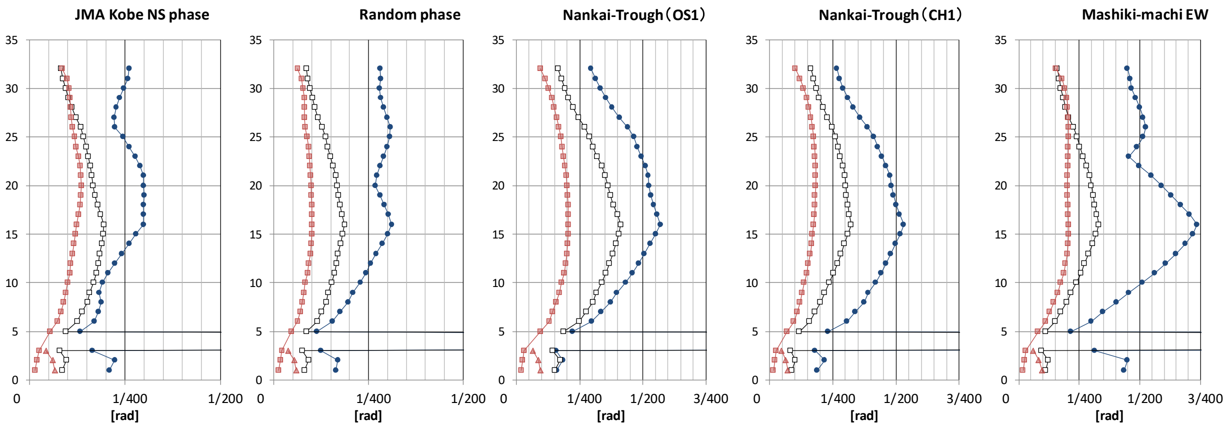

Fig. 12 Maximum response interlaminar deformation angle

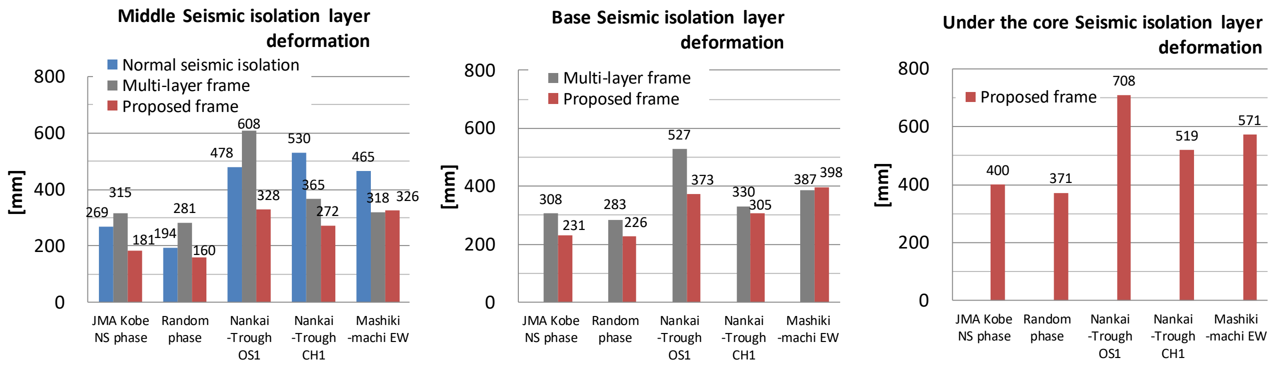

Fig. 13 Maximum response deformation of seismic isolation layers

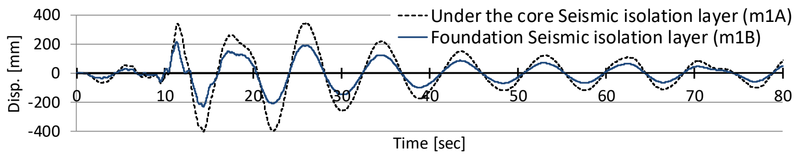

Fig. 14 Seismic isolation layer deformation at base part and core

5. Summary

In this paper, we propose a new frame structure consisting of multiple seismic isolation layers and a core wall with its own base isolation that penetrates the whole building. We have determined effective seismic isolation characteristics for the proposed frame and performed seismic response analysis using a multi-degree-of-freedom model constructed with these characteristics. The results of this work yield the following findings.

1. Increasing the damping under the core wall results in an increase in only the primary damping factor without causing overdamping of the secondary damping factor. This means that a significant response reduction effect can be expected in the resonance region compared to a multi-layer frame without a base-isolated core wall.
2. By setting the eigenvector ratios to $1.0 < \gamma < 2.0$, $\kappa > 1.0$, $\alpha \leqq 1.0$ for the stiffness ratio of each seismic isolation layer, it is possible to reduce the higher mode motion of the lower floors (mass point B).
3. The response of the proposed frame is less than 100 cm/s^2 and the seismic isolation layer deformation is less than the guaranteed deformation performance for ground motions based on a Level 2 earthquake.
4. In the future, we plan to conduct a study that includes a locking mechanism in order to suppress deformation of the seismic isolation layer in strong winds.

6. Acknowledgements

In preparing this paper, we used observation records from the Japan Meteorological Agency and Kumamoto Prefecture. We thank these organizations for publishing them.

7. References

[1] Building Research Institute: Publication of digital data for prediction of long-period and long-duration ground motions, Document No. 1, https://www.kenken.go.jp/japanese/information/information/press/2014/2_1.pdf, 2014 (in Japanese) (referred on 6 March, 2017)

[2] Architectural Institute of Japan (Symposium): Five years after the Great East Japan Earthquake – Achievements and remaining issues in architectural vibration engineering – 2016 (in Japanese)

[3] Yamamoto, M, Sone, T, Murata, K, Oshima, T, Yamamoto, K, Saito, Yamamoto, K (2015): Dynamic behavior of setback building with multiple isolation story (Parts 1-3). Architectural Institute of Japan, Annual Meeting, pp633-638, 2015.9 (in Japanese)

[4] Tsuji, M, Tsuji, C, Kataoka, N (2014): Seismic characteristics of multiple isolation building with plural isolation stories, Journal of Structural and Construction Engineering (Transactions of AIJ), No.705, pp.1613-1623, 2014.11(in Japanese)

[5] Suga, T, Kotsuki, S, Sugimoto, K, Minami, H, Fukukita, A (2016): Seismic isolation building with response control system (seismic response analysis of building with plural isolation layers and linked dampers), Architectural Institute of Japan, Annual Meeting, pp635-636, 2016.8 (in Japanese)

[6] Architectural Institute of Japan: Structural response and performance for long-period seismic ground motions, Architectural Institute of Japan, 2007 (in Japanese)

[7] Japan Meteorological Agency: http://www.data.jma.go.jp/svd/eqev/data/kyoshin/jishin/1604160125_kumamoto/

